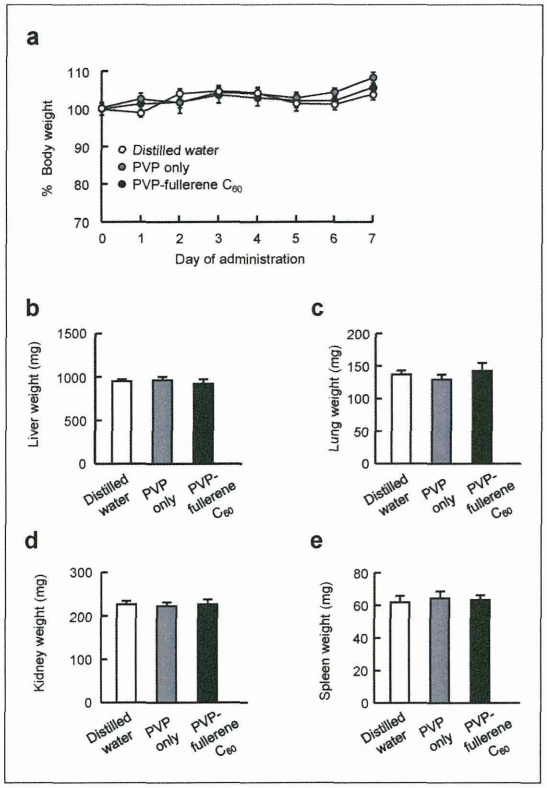

Fig. 1: *Effect of oral administration of PVP-fullerene C_{60} on body weight and wet organ weights of mice.* PVP-fullerene C_{60} solution in distilled water (50 mg/500 μL/mouse) was administrated orally. Control mice received distilled water or PVP only; all mice were treated by oral gavage daily for 7 d. (a) Body weight during oral administration of PVP-fullerene C_{60}, PVP only, or distilled water. Wet weight of (b) liver, (c) lung, (d) kidney, and (e) spleen after 7 d of treatment. Data are given as mean ± SEM (n = 8)

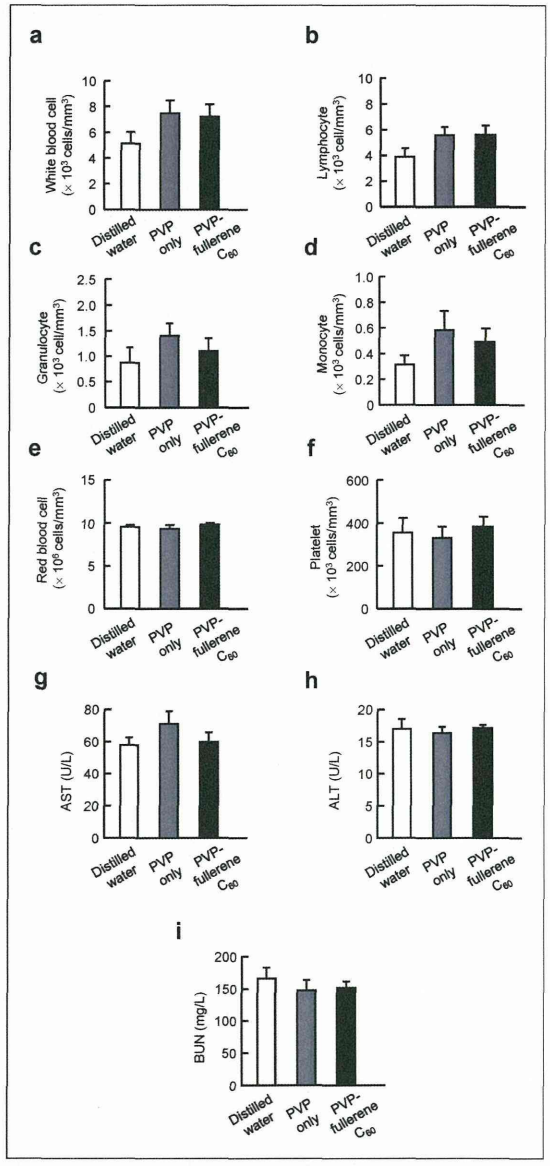

Fig. 2: *Effect of oral administration of PVP-fullerene C_{60} on hematologic and biochemical parameters of mice.* (a–f) Hematologic parameters were measured after oral administration of PVP-fullerene C_{60} for 7 d. (g–i) Biochemical parameters in the plasma were measured after oral administration of PVP-fullerene C_{60} for 7 d. Data are given as mean ± SEM (n = 6 or 7)

2. Investigations, results and discussion

We first used dynamic light scattering to measure the hydrodynamic diameters of PVP-fullerene C_{60}. The particle size of PVP-fullerene C_{60} in the distilled water was 127 nm, and its zeta potential was –2.2 mV.

To examine the safety of PVP-fullerene C_{60} after oral administration to mice, each mouse received 0.5 ml of distilled water, PVP only, or PVP-fullerene C_{60} solution by oral gavage once daily for 7 d. Daily behavior including eating, drinking, and activity did not differ between groups; no mice died; and there were no overt differences in body weight gain between groups (Fig. 1a). In addition, wet organ weight after 7 d of oral treatment did not differ significantly between groups (Fig. 1b–e). Hematologic parameters including numbers of red blood cells, platelets, white blood cells, lymphocytes, granulocytes, and monocytes in mice did not show significant differences between groups (Fig. 2a–f). Similarly, plasma biochemical parameters including aspartate aminotransferase (AST) and alanine aminotransferase (ALT) as indicators of hepatic injury and blood urea nitrogen (BUN) as a marker of renal damage did not differ significantly between groups (Fig. 2g–i).

Disease symptom scores and colon length are well-known indicators of colonic inflammation, which is the most common adverse effect after oral administration of test compounds. We scored fecal occult blood as a disease symptom in mice. Similar to those for the distilled water group (1.6 ± 0.1) or PVP only group (1.5 ± 0.1), the score for the PVP-fullerene C_{60}-treated group (1.5 ± 0.1) did not indicate any occult or gross rectal bleeding (Fig. 3a). Furthermore neither colon length (Fig. 3b) nor histology (Fig. 3c–e) differed between groups. Taking together all of our results, we consider that oral administration of 50 mg PVP-fullerene C_{60} daily for 7 d has negligible effects on the health of the colon in mice (Fig. 3).

Various *in vitro* and *in vivo* safety assessments of fullerene C_{60} and its derivatives have been reported previously (Metanawin et al. 2011; Nielsen et al. 2008; Zhang et al. 2009). Most studies have shown that fullerene C_{60} and its derivatives are not genotoxic under *in vitro* conditions (Aoshima et al. 2010; Ema

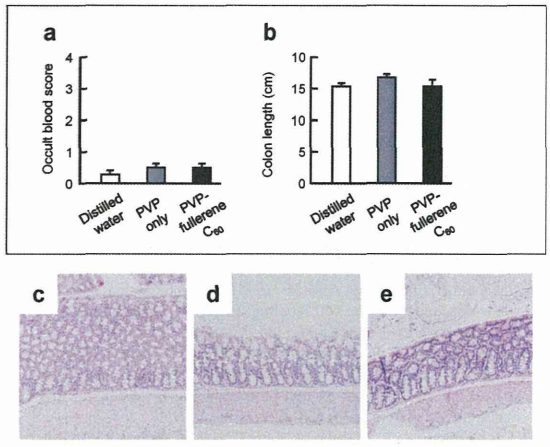

Fig. 3: Effect of oral administration of PVP-fullerene C_{60} on the histology of the colon in mice. (a) Occult blood scores were determined after 7 d of treatment by assessing the consistency, overt blood, and occult blood of feces. (b) Effect of PVP-fullerene C_{60} on colon length. All data are expressed as mean ± SEM (n = 8). Histopathology of the distal colon in C57/BL6 mice after oral administration of distilled water (c), PVP only (d) or PVP-fullerene C_{60} (e) for 7 d. Representative sections were stained with hematoxylin and eosin and examined by using light microscopy

et al. 2012; Shinohara et al. 2009). In addition, water-soluble fullerene C_{60} derivatives can safely be used for dermal and intraperitoneal injection (Aoshima et al. 2010; Gharbi et al. 2005). However, insufficient information is available regarding the safety of water-soluble fullerene C_{60} derivatives after oral administration. In this study, we evaluated the safety and toxicity of oral PVP-fullerene C_{60} by monitoring the body weight, hematologic and biochemical parameters, and colonic health of treated mice. Our results indicate that oral PVP-fullerene C_{60} has no adverse effects on the evaluated parameters in mice.

Guidelines from the Organization for Economic Co-operation and Development (OECD) recommend 28- and 90-d repeated-dose oral toxicity studies in rodents for the safety assessment of chemicals used as nanomaterials. As a first step in the safety assessment of PVP-fullerene C_{60}, we here performed a 7-d oral toxicity study. Now we are trying to perform safety evaluations after long-term exposure.

In conclusion, we showed that oral administration of PVP-fullerene C_{60} induced negligible change in various hematologic, biochemical, and histologic parameters in mice. Although additional studies are needed to further examine the safety of PVP-fullerene C_{60}, we consider that our data provide the basic information that likely will facilitate the development of safe and effective forms of fullerene C_{60}.

3. Experimental

3.1. Particles

PVP-fullerene C_{60} was provided by Vitamin C60 BioResearch (Tokyo, Japan) and is composed of purified fullerene C_{60} and PVP of 60 to 80 kDa. The C_{60} content in PVP-fullerene C_{60} was determined by HPLC analysis on a 5PBB column (Nacalai Tesque, Kyoto, Japan) and found to be approximately 3000 ppm. PVP-fullerene C_{60} was used after 5 min of sonication (280 W output; Ultrasonic Cleaner, AS One, Tokyo, Japan) and 1 min of vortexing. Particle size and zeta potential were measured by using a Zetasizer Nano-ZS (Malvern Instruments, Worcestershire, UK). The mean size and size distribution of particles were measured by using dynamic light scattering; zeta potential was measured by using laser doppler electrophoresis.

3.2. Mice

Female C57BL/6 mice were purchased from Nippon SLC (Kyoto, Japan) and used at 6 weeks of age. Mice were housed in a ventilated animal room maintained at 20 ± 2 °C with a 12:12-h light:dark cycle. Distilled water and sterilized mouse chow were available *ad libitum*. All procedures were performed in accordance with institutional ethical guidelines for animal experiments. During the treatment period, each mouse received 0.5 ml distilled water, PVP only, or PVP-fullerene C_{60} in distilled water (total dose, 50 mg) by oral gavage once daily for 7 d. Mice were euthanized 24 h after administration of the final dose, and liver, lung, kidney, and spleen tissues were harvested and weighed. Blood samples were collected in tubes containing 5 IU/ml heparin sodium, and plasma was harvested. Colons were resected for the determination of colon length (from cecum to anus) and histopathologic examination. Feces were collected and evaluated for occult blood.

3.3. Hematologic analysis

The numbers of white blood cells, granulocytes, lymphocytes, monocytes, red blood cells, and platelets in whole blood were measured by using an auto analyzer (VetScan HMII Hematology System, Abaxis, Union City, CA). Liver function was assessed by measuring plasma levels of AST and ALT. Nephrotoxicity was evaluated by measuring plasma levels of BUN. AST, ALT, and BUN were assayed by using a biochemical autoanalyzer (Fuji Dri-Chem 7000, Fujifilm, Tokyo, Japan).

3.4. Histopathologic examination

For histology of paraffin-fixed tissue, colons were excised and fixed overnight in 10% neutral buffered formalin, embedded in paraffin blocks, sliced, and placed on glass slides. Sections were deparaffinized, rehydrated through a graded series of ethanol, and stained with hematoxylin and eosin. Stained sections were dehydrated through a graded ethanol series and mounted using permount (OCT Compound, Sakura Finetek, Tokyo, Japan). Representative histologic images were recorded by a CCD digital camera that was affixed to a microscope. Fecal occult blood was scored by using the Coloscreen Occult Blood Card Test (Shionogi, Osaka, Japan), with the scale ranging from 0 for negative to 4 for strongly positive.

3.5. Statistical analysis

All results are presented as mean ± standard error of the mean (SEM). Statistical significance in differences was evaluated by analysis of variance (ANOVA) followed by Bonferroni correction. The P value used to define significance ($P < 0.05$).

Competing interests: The authors declare that there are no conflicts of interest.

Acknowledgements: This study was supported in part by Grants-in-Aid for Scientific Research from the Ministry of Education, Culture, Sports, Science and Technology of Japan (MEXT), and from the Japan Society for the Promotion of Science (JSPS); and by a the Knowledge Cluster Initiative (MEXT); by Health Labour Sciences Research Grants from the Ministry of Health, Labor and Welfare of Japan (MHLW); by a Global Environment Research Fund from Minister of the Environment; by Food Safety Commission (Cabinet Office); by The Cosmetology Research Foundation; by The Smoking Research Foundation; by The Takeda Science Foundation; by The Nagai Foundation Tokyo; by The Research Foundation for Pharmaceutical Sciences; and by The Japan Food Chemical research Foundation.

References

Aoshima H, Kokubo K, Shirakawa S, Ito M, Yamana S, Oshima T (2009) Antimicrobial activity of fullerenes and their hydroxylated derivatives. Biocontrol Sci 14: 69–72.

Aoshima H, Yamana S, Nakamura S, Mashino T (2010) Biological safety of water-soluble fullerenes evaluated using tests for genotoxicity, phototoxicity, and pro-oxidant activity. J Toxicol Sci 35: 401–409.

Augustin MA, Sanguansri P (2009) Nanostructured materials in the food industry. Adv Food Nutr Res 58: 183–213.

Benn TM, Westerhoff P, Herckes P (2011) Detection of fullerenes (C60 and C70) in commercial cosmetics. Environ Pollut 159: 1334–1342.

Bimbo LM, Sarparanta M, Santos HA, Airaksinen AJ, Makila E, Laaksonen T, Peltonen L, Lehto VP, Hirvonen J, Salonen J (2010) Biocompatibility of thermally hydrocarbonized porous silicon nanoparticles and their biodistribution in rats. ACS Nano 4: 3023–3032.

Bowman DM, van Calster G, Friedrichs S (2010) Nanomaterials and regulation of cosmetics. Nat Nanotechnol 5: 92.

Chen Z, Ma L, Liu Y, Chen C (2012) Applications of functionalized fullerenes in tumor theranostics. Theranostics 2: 238–250.

Ema M, Tanaka J, Kobayashi N, Naya M, Endoh S, Maru J, Hosoi M, Nagai M, Nakajima M, Hayashi M, Nakanishi J (2012) Genotoxicity evaluation of fullerene C60 nanoparticles in a comet assay using lung cells of intratracheally instilled rats. Regul Toxicol Pharmacol 62: 419–424.

Gharbi N, Pressac M, Hadchouel M, Szwarc H, Wilson SR, Moussa F (2005) [60]fullerene is a powerful antioxidant in vivo with no acute or subacute toxicity. Nano Lett 5: 2578–2585.

Hu Z, Liu S, Wei Y, Tong E, Cao F, Guan W (2007) Synthesis of glutathione C60 derivative and its protective effect on hydrogen peroxide-induced apoptosis in rat pheochromocytoma cells. Neurosci Lett 429: 81–86.

Kato S, Aoshima H, Saitoh Y, Miwa N (2009) Biological safety of Lipo-Fullerene composed of squalane and fullerene-C60 upon mutagenesis, photocytotoxicity, and permeability into the human skin tissue. Basic Clin Pharmacol Toxicol 104: 483–487.

Kato S, Taira H, Aoshima H, Saitoh Y, Miwa N (2010) Clinical evaluation of fullerene-C60 dissolved in squalane for anti-wrinkle cosmetics. J Nanosci Nanotechnol 10: 6769–6774.

Kokubo K, Tochika S, Kato M, Sol Y, Oshima T (2008) AlCl3-catalyzed tandem acetylation of hydroarylated [60]fullerenes. Org Lett 10: 3335–3338.

Konstantatos G, Sargent EH (2010) Nanostructured materials for photon detection. Nat Nanotechnol 5: 391–400.

Krusic PJ, Wasserman E, Keizer PN, Morton JR, Preston KF (1991) Radical reactions of c60. Science 254: 1183–1185.

Lin CM, Lu TY (2012) C60 Fullerene Derivatized Nanoparticles and their Application to Therapeutics. Recent Pat Nanotechnol 6: 105–113.

Metanawin T, Tang T, Chen R, Vernon D, Wang X (2011) Cytotoxicity and photocytotoxicity of structure-defined water-soluble C60/micelle supramolecular nanoparticles. Nanotechnology 22: 235604.

Nielsen GD, Roursgaard M, Jensen KA, Poulsen SS, Larsen ST (2008) In vivo biology and toxicology of fullerenes and their derivatives. Basic Clin Pharmacol Toxicol 103: 197–208.

Petros RA, DeSimone JM (2010) Strategies in the design of nanoparticles for therapeutic applications. Nat Rev Drug Discov 9: 615–627.

Shinohara N, Matsumoto K, Endoh S, Maru J, Nakanishi J (2009) In vitro and in vivo genotoxicity tests on fullerene C60 nanoparticles. Toxicol Lett 191: 289–296.

Xiao L, Matsubayashi K, Miwa N (2007) Inhibitory effect of the water-soluble polymer-wrapped derivative of fullerene on UVA-induced melanogenesis via downregulation of tyrosinase expression in human melanocytes and skin tissues. Arch Dermatol Res 299: 245–257.

Yamago S, Tokuyama H, Nakamura E, Kikuchi K, Kananishi S, Sueki K, Nakahara H, Enomoto S, Ambe F (1995) In vivo biological behavior of a water-miscible fullerene: 14C labeling, absorption, distribution, excretion and acute toxicity. Chem Biol 2: 385–389.

Yin JJ, Lao F, Fu PP, Wamer WG, Zhao Y, Wang PC, Qiu Y, Sun B, Xing G, Dong J, Liang XJ, Chen C (2009) The scavenging of reactive oxygen species and the potential for cell protection by functionalized fullerene materials. Biomaterials 30: 611–621.

Yudoh K, Karasawa R, Masuko K, Kato T (2009a) Water-soluble fullerene (C60) inhibits the development of arthritis in the rat model of arthritis. Int J Nanomedicine 4: 217–225.

Yudoh K, Karasawa R, Masuko K, Kato T (2009b) Water-soluble fullerene (C60) inhibits the osteoclast differentiation and bone destruction in arthritis. Int J Nanomedicine 4: 233–239.

Zhang LW, Yang J, Barron AR, Monteiro-Riviere NA (2009) Endocytic mechanisms and toxicity of a functionalized fullerene in human cells. Toxicol Lett 191: 149–157.

ORGANIC LETTERS

2012
Vol. 14, No. 23
6040–6043

Facile and Exclusive Formation of Aziridinofullerenes by Acid-catalyzed Denitrogenation of Triazolinofullerenes

Naohiko Ikuma,* Tsubasa Mikie, Yuta Doi, Koji Nakagawa, Ken Kokubo, and Takumi Oshima*

Division of Applied Chemistry, Graduate School of Engineering, Osaka University, 2-1 Yamadaoka, Suita, Osaka 565-0871, Japan

ikuma@chem.eng.osaka-u.ac.jp, oshima@chem.eng.osaka-u.ac.jp

Received October 24, 2012

ABSTRACT

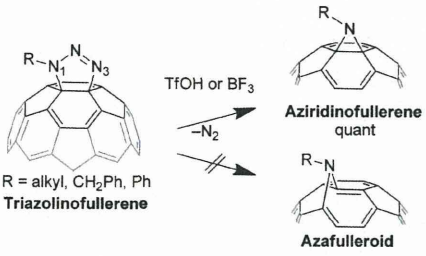

Variously substituted [6,6]closed aziridinofullerenes were exclusively obtained from acid-catalyzed denitrogenation of triazolinofullerenes without formation of relevant [5,6]open azafulleroids, which are the major products on noncatalyzed denitrogenation. The mechanistic consideration by DFT calculations suggested a reaction sequence involving initial pre-equilibrium protonation of the triazoline N_1 atom, generation of aminofullerenyl cation by nitrogen-extrusion, and final aziridination.

Aziridinofullerenes, bearing a strained aziridine ring, are useful synthetic intermediates for highly efficient and regioselective addition of spherical fullerene cages, such as acid-induced 1,4-bisaddition of aromatic compounds,[1,2] [2 + 2] cycloaddition with alkynes,[2] and isomerization to azafulleroids.[1b,3] The aziridinofullerenes have been hitherto widely prepared by 1,3-dipolar cycloaddition of azides to C_{60}, followed by thermal or photochemical denitrogenation of the triazolinofullerene adducts.[4] Although some new synthetic methods of certain aziridinofullerenes by nucleophilic addition of chloramines,[1] iminophenyliodinanes,[2] sulfilimines[3] and *N*,*N*-dihalosulfonamides[5] were recently reported, the classical denitrogenation of labile triazolinofullerenes is still a useful procedure for the introduction of various substituents and functional groups R at the triazoline N_1 position such as amino acids,[6] saccharides[7] and lipid substituents.[8] However, the thermal denitrogenation has some difficulty in controlling the reaction conditions and also preventing the formation of major concomitant [5,6]open azafulleroids.[4,9,10] In this context, it is eagerly desired to find an efficient aziridination reaction and hence

(1) (a) Minakata, S.; Tsuruoka, R.; Nagamachi, T.; Komatsu, M. *Chem. Commun.* **2008**, 323–325. (b) Tsuruoka, R.; Nagamachi, T.; Murakami, Y.; Komatsu, M.; Minakata, S. *J. Org. Chem.* **2009**, *74*, 1691–1697.

(2) Nambo, M.; Segawa, Y.; Itami, K. *J. Am. Chem. Soc.* **2011**, *133*, 2402–2405.

(3) (a) Nakahodo, T.; Okada, M.; Morita, H.; Yoshimura, T.; Ishitsuka, M. O.; Tsuchiya, T.; Maeda, Y.; Fujihara, H.; Akasaka, T.; Gao, X.; Nagase, S. *Angew. Chem., Int. Ed.* **2008**, *47*, 1298–1300. (b) Okada, M.; Nakahodo, T.; Ishitsuka, M. O.; Nikawa, H.; Tsuchiya, T.; Akasaka, T.; Fujie, T.; Yoshimura, T.; Slanina, Z.; Nagase, S. *Chem. Asian J.* **2010**, *6*, 416–423.

(4) (a) Prato, M.; Li, Q. C.; Wudl, F.; Lucchini, V. *J. Am. Chem. Soc.* **1993**, *115*, 1148–1150. (b) Grosser, T.; Prato, M.; Lucchini, V.; Hirsch, A.; Wudl, F. *Angew. Chem., Int. Ed.* **1995**, *34*, 1343–1345. (c) Averdung, J.; Mattay, J. *Tetrahedron* **1996**, *52*, 5407–5420. (d) Shen, C. K. F.; Yu, H.-H.; Juo, C.-G.; Chien, K.-M.; Her, G.-R.; Luh, T.-Y. *Chem.—Eur. J.* **1997**, *3*, 744–748. (e) Wu, R.; Lu, X.; Zhang, Y.; Zhang, J.; Xiong, W.; Zhu, S. *Tetrahedron* **2008**, *64*, 10694–10698.

(5) Nagamachi, T.; Takeda, Y.; Nakayama, K.; Minakata, S. *Chem.—Eur. J.* **2012**, *18*, 12035–12045.

(6) Strom, T. A.; Barron, A. R. *Chem. Commun.* **2010**, *46*, 4764–4766.

(7) Kato, H.; Yashiro, A.; Mizuno, A.; Nishida, Y.; Kobayashi, K.; Shinohara, H. *Bioorg. Med. Chem. Lett.* **2001**, *11*, 2935–2939.

(8) (a) Murakami, H.; Watanabe, Y.; Nakashima, N. *J. Am. Chem. Soc.* **1996**, *118*, 4484–4485. (b) Nakanishi, T.; Morita, M.; Murakami, H.; Sagara, T.; Nakashima, N. *Chem.—Eur. J.* **2002**, *8*, 1641–1648. (c) Murakami, H.; Nakanishi, T.; Morita, M.; Taniguchi, N.; Nakashima, N. *Chem. Asian J.* **2006**, *1*, 860–867.

10.1021/ol302928d
Published on Web 11/27/2012

we have applied possible acid-catalyzed denitrogenation of usual triazoline compounds.[11] Here, we present the successful and exclusive formation of [6,6]closed aziridinofullerenes from simple Brønsted/Lewis acid-catalyzed denitrogenation of triazolinofullerenes.

The preparation of various triazolinofullerenes **1a–f** is described in Table 1. For the sake of safety, the employed alkyl azides were prepared from alkyl halides with sodium azide in acetonitrile, and then immediately used *in situ* for the subsequent 1,3-dipolar cycloaddition by adding C_{60} solution in *o*-dichlorobenzene (*o*-DCB) at elevated temperature (~50 °C). To reduce the multiaddition, the reaction was ceased at the 60–70% consumption of C_{60} (12–36 h) except for the syntheses of **1e** and **1f**, which were prepared at room temperature for the prolonged reaction time (96 h) to suppress the unfavorable thermal denitrogenation into the corresponding azafulleroids. The yields of **1a–f** were comparable with those of the previous syntheses of triazolinofullerenes.[4] All triazolinofullerenes were fully identified with $^1H/^{13}C$–NMR and HRMS spectrometry.

Table 1. Synthesis of Aziridinofullerenes **2a–f** via Acid-induced Denitrogenation of Triazolinofullerenes **1a–f**

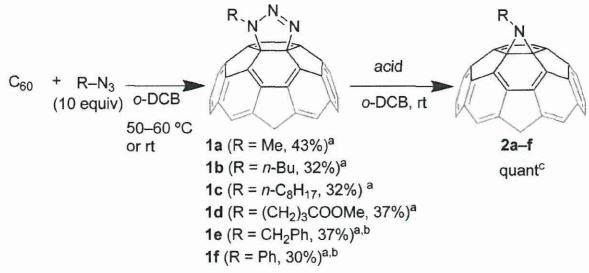

entry	reactant	acid[d]	time (h)	conv (%)
1	**1a**	TfOH	<0.1	100
2	**1a**	CH_3SO_3H	0.5	100
3	**1a**	CF_3COOH	24	0
4	**1a**	BF_3	0.5	100
5	**1a**	BF_3[e]	3	81
6	**1a**	$B(C_6H_5)_3$	5	100
7	**1a**	$AlCl_3$	24	0
8	**1a**	$TiCl_4$	24	0
9	**1b**	TfOH	0.1	100
10	**1c**	TfOH	0.1	100
11	**1d**	TfOH	0.1	100
12	**1e**	TfOH (0.5 equiv)	0.1	100
13	**1f**	TfOH (1.0 equiv)	0.1	100

[a] Isolated yield. [b] At rt. [c] >95% isolated yield. [d] Unless otherwise noted, 0.1 equiv of acid was used. [e] Toluene solvent.

Acid-catalyzed denitrogenation of variously alkyl-substituted **1a–e** readily occurred on addition of catalytic ammounts (0.1–0.5 equiv) of superacid CF_3SO_3H (TfOH) and Lewis acid BF_3 (Table 1).[12] For phenyl-substituted **1f**, an equivalent amount of TfOH was needed to complete the denitrogenation (entry 13), probably because of the far more reduced basicity of the phenyl-sustituted N_1-atom than that of alkyl-substituted one. Noticeably, the [6,6]closed aziridinofullerenes **2a–f** were exclusively obtained with no appreciable amount of [5,6]open azafulleroids as exemplified for the denitrogenation of **1a** under BF_3 (Figure 1). The C_{2v} symmetric structures of **2a–f** were fully characterized by $^1H/^{13}C$–NMR spectroscopy (Supporting Information).

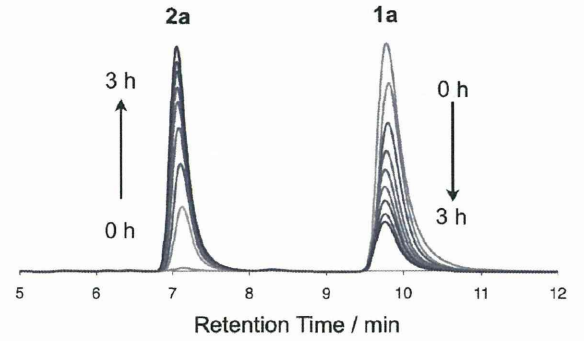

Figure 1. HPLC trace of denitrogenation of **1a** into **2a** by BF_3 in toluene (cf. Table 1, entry 5).

It was also found that the denitrogenation rates of triazolinofullerens **1a–f** by several Brønsted/Lewis acids depend on their acidities (Table 1). The weaker CH_3SO_3H needed longer reaction time (0.5h) than CF_3SO_3H (entries 1 and 2), and much weaker CF_3COOH was ineffective (entry 3). BF_3 was found to more efficiently cause the denitrogenation than $B(C_6F_5)_3$ (entries 4 and 6), but no reaction occurred with $AlCl_3$ and $TiCl_4$ (entries 7 and 8). These results suggest the protonation (or coordination of Lewis acids) at the basic triazoline N_1 atom would be a key step of the denitrogenation (*vide infra*). In fact, the reaction was accelerated with increasing solvent polarity as seen in a

(9) Although addition of nitrenes by denitrogenation of azides gave aziridinofullerenes with relatively high yields, their substituents were limited to carbonyl/sulfonyl compounds. See: (a) Banks, M.; Cadogan, J.; Gosney, I.; Hodgson, P.; Langridgesmith, P.; Millar, J.; Taylor, A. *Tetrahedron Lett.* **1994**, *35*, 9067–9070. (b) Smith, A. B.; Tokuyama, H. *Tetrahedron* **1996**, *52*, 5257–5262. (c) Ulmer, L.; Mattay, J. *Eur. J. Org. Chem.* **2003**, 2933–2940.

(10) Exceptionally, the reaction of hydrazoic acid with C_{60} gave aziridinofullerene, as recently reported by Akhmetov *et al.* In the light of our results and discussion in this paper, one can suppose that the excess amount of sulfuric acid used for *in situ* preparation of hydrazoic acid causes the formation of aziridinofullerene. See: Akhmetov, A. R.; Tuktarov, A. R.; Dzhemilev, U. M.; Yarullin, I. R.; Gabidullina, L. A. *Russ. Chem. Bull.* **2011**, *60*, 1885–1887.

(11) (a) Mishchenko, A.; Prosyanik, A.; Belov, P.; Romanchenko, V.; Belova, Y.; Markov, V. *Khim Geterotsikl. Soedinenii* **1984**, 338–342. *Chem. Heterocycl. Compd.* **1984**, *20*, 270–274. (b) Wladkowski, B. D.; Smith, R. H.; Michejda, C. J. *J. Am. Chem. Soc.* **1991**, *113*, 7893–7897. (c) Smith, R. H.; Wladkowski, B. D.; Taylor, J. E.; Thompson, E. J.; Pruski, B.; Klose, J. R.; Andrews, A. W.; Michejda, C. J. *J. Org. Chem.* **1993**, *58*, 2097–2103. (d) Rozhkov, V.; Voznesenskii, V.; Kostyanovsky, R. *Russ. Chem. Bull.* **1998**, *47*, 115–118. (e) Prosyanik, A.; Rozhkov, V.; Moskalenko, A.; Mishchenko, A.; Forni, A.; Moretti, I.; Torre, G.; Brukner, S.; Malpezzi, L.; Kostyanovsky, R. *Russ. Chem. Bull.* **1998**, *47*, 119–126. (f) Benati, L.; Calestani, G.; Nanni, D.; Spagnolo, P. *J. Org. Chem.* **1998**, *63*, 4679–4684. (g) Troyer, T. L.; Muchalski, H.; Hong, K. B.; Johnston, J. N. *Org. Lett.* **2011**, *13*, 1790–1792.

(12) An excess amount of acid in toluene led to further reaction, probably electrophilic arylation of aziridinofullerene as previously reported in refs 1b and 2.

plot of log k vs solvent polarity parameter E_T (Figure 2),[13,14] probably because of the stabilization of such polar acid–base complexes.

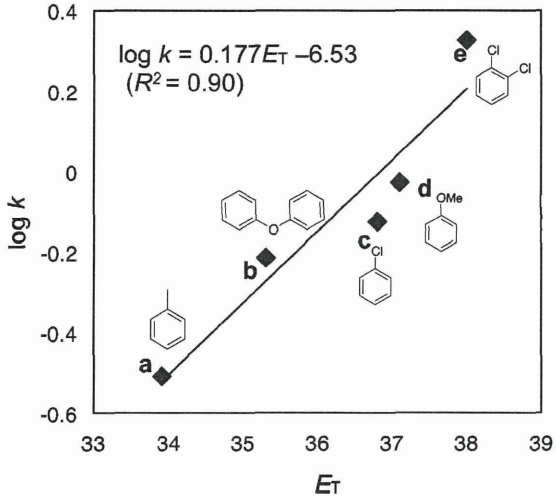

Figure 2. Plot of log k vs solvent polarity parameter E_T for the reaction of **1a** with BF_3[13]

Why does the present acid-catalyzed condition exclusively provide the [6,6]closed aziridinofullerene in contrast to the thermal denitrogenation? Thermal condition has been well-known to prefer the formation of [5,6]open azafulleroid via the possible three pathways: (1) concerted, (2) ionic stepwise and (3) radical stepwise.[4d,e,15] A DFT calculation (B3LYP/6-31G(d))[16] with solvent parameters (IEFPCM, *o*-dichlorobenzene) suggested a concerted-like transition state **1a**-TS (Scheme 1, path a, and Figure 3b) as previously reported for its carbon analog, pyrazolinofullerene.[17] The barrier energy (34.3 kcal/mol) for the denitrogenation of **1a** is lower than those of previously reported two types of ionic transition states (N_1–N_2 or N_3–C_1 cleavage) by AM1 calculations (46.8 and 45.2 kcal/mol, respectively).[15] Moreover, the calculation of inherent reaction coordinate (IRC) showed the sp^2-like N_1 atom considerably approached the C_2 atom (purple cross in Figure 3a), implying enhanced aza-bridging over the 5,6-conjunct bond. The optimization of the forward-edge structure of the IRC calculation showed transient [5,6]closed aziridinofullerene **3a** capable of undergoing labile valence isomerization to [5,6]open azafulleroid **4a** (Scheme 1 and Figure 3c). This computational result

(13) The 0.1 equiv of BF_3 was used (1.29×10^{-3} M). The k value in toluene is 0.310 M^{-1} s^{-1} and the relative k values in other solvents are 1.97 (**b**), 2.42 (**c**), 3.03 (**d**), and 6.84 (**e**), respectively.

(14) Reichardt, C. *Chem. Rev.* **1994**, *94*, 2319–2358.

(15) Cases, M.; Duran, M.; Mestres, J.; Martín, N.; Solà, M. *J. Org. Chem.* **2001**, *66*, 433–442.

(16) All DFT calculations were carried out with *Gaussian 09* software. Its full citation is shown in Supporting Information.

(17) Wallenborn, E.; Haldimann, R.; Klarner, F.; Diederich, F. *Chem.—Eur. J.* **1998**, *4*, 2258–2265.

Scheme 1. Suggested (a) Thermal and (b) TfOH-catalytic Pathways with Calculated Energies (B3LYP/6-31G(d) with Solvent Parameter), which are Relative to the Heat of Formation of **1a** (for Thermal) and the Summation of Those of **1a** and TfOH (for Acid-catalyzed)

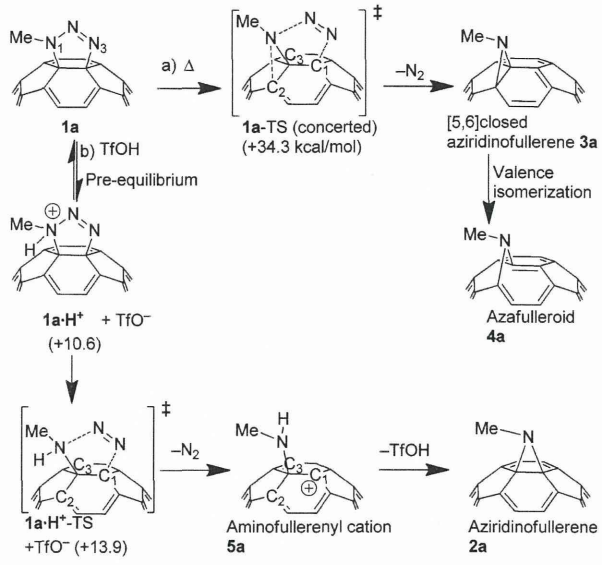

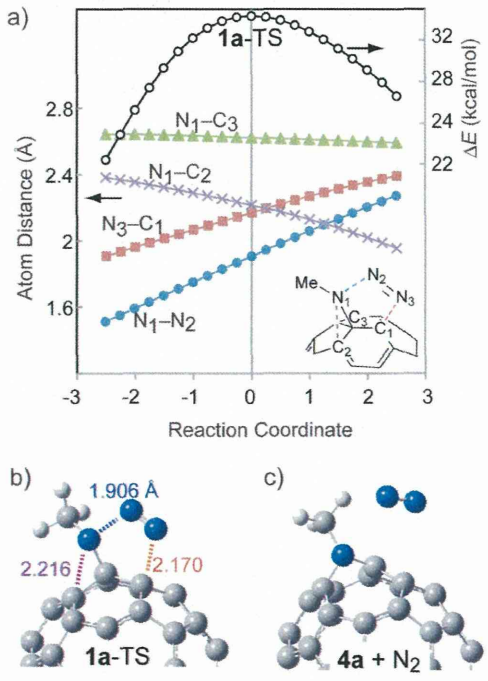

Figure 3. (a) Energies and atomic distances of IRC calculation (B3LYP/6-31G(d) with solvent parameters) for the thernal denitrogenation of **1a**. The energies are relative to the initial state **1a**. (b) Geometry of the concerted transition state **1a**-TS. (c) Geometry of [5,6]open **4a** (and N_2) derived from the optimization of the IRC forward-edge structure (s = 2.50).

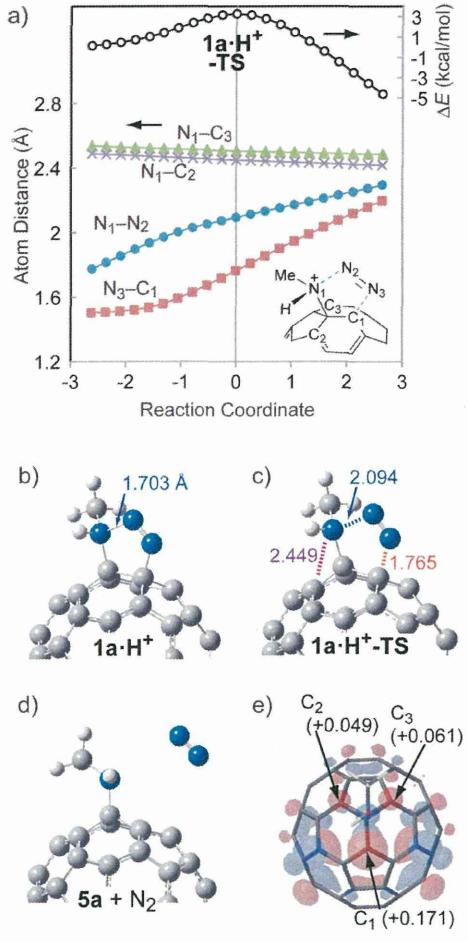

Figure 4. (a) Energies and atomic distances of IRC calculation (B3LYP/6-31G(d) with solvent parameters) for the acid-catatytic denitrogenation. The energies are relative to the initial state **1a**·H^+. (b) Geometry of N_1-acidified **1a**·H^+. (c) Transition state geometry (**1a**·H^+-TS) of denitrogenation of **1a**·H^+. (d) Geometry of aminofullerenyl cation **5a** (and N_2) derived from the optimization of the IRC forward-edge structure (s = 2.64). (e) LUMO orbital distribution and natural bonding orbital charge (in parentheses) of the ionic intermediate **5a**.

obviously conforms with the selective formation of azafulleroids on usual thermal conditions.

(18) Although the triazoline N_3 atom would be more easily protonated, such N_3-protonated species does not lead to the denitrogenation (see, ref 11b).

(19) (a) Yang, C.; Cho, S.; Heeger, A. J.; Wudl, F. *Angew. Chem., Int. Ed.* **2009**, *48*, 1592–1595. (b) Park, S. H.; Yang, C.; Cowan, S.; Lee, J. K.; Wudl, F.; Lee, K.; Heeger, A. J. *J. Mater. Chem.* **2009**, *19*, 5624–5628.

By contrast, TfOH can protonate an N_1 atom to give triazolinium intermediate **1a**·H^+ with a long N_1–N_2 distance (1.7 Å) (Scheme 1, path b, and Figure 4b).[18] A transition state calculation of denitrogenation of **1a**·H^+ showed far more lower barrier energy (3.3 kcal, Figure 4c) than that of the thermal reaction (34.3 kcal). In contrast to the case of thermal condition, the distance between the sp^3-like ammonium N_1 and C_2 (or C_3) is little changed by the IRC calculation, due to the absence of potential N_1 lone pair electrons (Figure 4a). Furthermore, the optimization of the IRC forward-edge structure resulted in aminofullerenyl cation **5a**, with N_1 being located almost perpendicular to the C_1–C_2–C_3 plane (Scheme 1 and Figure 4d). The higher LUMO coefficient and/or positive natural bonding charge on C_1 (relative to C_2 and C_3) by a DFT calculation would be responsible for the formation of [6,6]closed aziridinofullerene. The total barrier energy of the rate-determing protonation (10.6 kcal/mol) and the fast denitrogantation (3.3) is still less than the half of the thermal denitrogenation (34.3), so that the acid-catalyzed reaction seems to proceed very soomthly at room temperature and exclusively provide [6,6]closed aziridinofullerenes.

In conclusion, synthetically useful aziridinofullerenes were exclusively obtained from simple acid-catalyzed denitrogenation of triazolinofullerenes, and the DFT calculations suggested a possible mechanism involving the initial protonation at the N_1 atom, followed by denitrogenation into the aminofullerenyl cation, and the final aziridination. This effective synthetic method would open a way to more versatile and regioselective functionalization of fullerenes directed to photovoltaic materials[5,19] and biological applications.[7]

Acknowledgment. This work was partly supported by Grant-in-Aid for Young Scientist (B) (No. 24750039) from Japan Society for the Promotion of Science (JSPS), and by Health Labour Sciences Research Grants from the Ministry of Health, Labour and Welfare of Japan (MHLW)

Supporting Information Available. General procedure for the reaction and identification of compounds by ^1H, ^{13}C NMR spectra, and FAB/MALDI-MS of **1a**–**f** and **2a**–**f**, and calculational results (energy, imaginary frequency and coordinates). This material is available free of charge via the Internet at http://pubs.acs.org.

The authors declare no competing financial interest.

Nanoscale

RSC Publishing

PAPER

Synthesis of a new class of fullerene derivative $Li^+@C_{60}O^-(OH)_7$ as a "cation-encapsulated anion nanoparticle"†

Cite this: *Nanoscale*, 2013, **5**, 2317

Hiroshi Ueno,[a] Ken Kokubo,*[a] Eunsang Kwon,[b] Yuji Nakamura,[a] Naohiko Ikuma[a] and Takumi Oshima[a]

Metal encapsulation into a cage and chemical modification on the outer surface of fullerenes endow them with some unique characteristic properties. Although the derivatization of endohedral fullerenes holds promise for producing novel new nano-carbon materials, there are few reports about such compounds. Herein, we report the synthesis of lithium encapsulated fullerenol $Li^+@C_{60}O^-(OH)_7$ using a fuming sulfuric acid method from $[Li^+@C_{60}](PF_6^-)$ and characterization of its structure by IR, NMR, FAB mass spectroscopy, and elemental analysis. The hydroxylation of $[Li^+@C_{60}](PF_6^-)$ is site-selective to preferentially give a single isomer (*ca.* 70%) with two minor isomers in marked contrast to the reaction of empty C_{60}. We conclude from the analysis of radical species produced in the reaction of a C_{60} cage with fuming sulfuric acid that this unusual site-selective hydroxylation is caused by the lower HOMO level of $Li^+@C_{60}$ than that of empty C_{60}. Furthermore, our results clearly indicate that the internal lithium cation is interacted with the introduced hydroxyl groups, and thus the properties of endohedral fullerenes can be controlled by the external modification of a fullerene cage.

Received 12th November 2012
Accepted 3rd January 2013

DOI: 10.1039/c3nr33608e

www.rsc.org/nanoscale

Introduction

Since the first report of macroscopic synthesis, complete isolation, and structural determination of lithium encapsulated fullerene $[Li^+@C_{60}](SbCl_6^-)$,[1] it has attracted growing attention owing to the strong electron accepting ability as well as the semiconducting property in the fields of organic electronics and materials chemistry.[2] However, details on the chemical modification of a fullerene cage and on the properties of resulting derivatives have not been well investigated except for the recent successful synthesis of $[Li^+@PCBM](PF_6^-)$.[3] Such external functionalization of endohedral metallofullerenes, especially solubilization in polar solvents, can be a versatile and promising protocol for controlling the physicochemical properties and the static behavior of encapsulated metal ions in a π-conjugated molecular cage.

On the other hand, polyhydroxylated fullerene, so-called fullerenol $C_{60}(OH)_n$, has been one of the most intriguing fullerene-based materials due to the prominent hydrophilicity and bioactivities with relatively low toxicity.[4–8] Various types of synthetic procedures for variously hydroxylated fullerenols[9–13] have been reported so far including our highly hydroxylated $C_{60}(OH)_{36}$ and $C_{60}(OH)_{44}$.[14,15] As expected, these fullerenols consist of a mixture of a wide variety of isomers with various numbers and positions of introduced hydroxyl groups, and only an average number of hydroxyl groups can be determined by elemental analysis except for recently synthesized $C_{60}(OH)_8$ as a single isomer.[16]

Considering these situations, it is no doubt that metal encapsulated fullerenols will play a significant role as a new class of functionalized nanomaterials not only in life science but also in materials chemistry. However, only a few cases are known; *e.g.*, Gd-encapsulated fullerene[17,18] and our previously reported mixture of Li-encapsulated and empty fullerenols prepared from the $Li@C_{60}$ cluster with an encapsulation ratio of only 12%.[19]

Herein, we report the unusual site-selective synthesis of Li-encapsulated fullerenol $Li^+@C_{60}O^-(OH)_7$ as a single major isomer along with two minor isomers when pure $[Li^+@C_{60}](PF_6^-)$ was treated with fuming sulfuric acid. Although the regiochemical positions of hydroxyl groups could not be determined due to its C_1 symmetrical structure, its unique physicochemical properties based on both the internal Li^+ and the external –OH groups as well as the mechanistic aspects on site-selective hydroxylation were revealed.

Results and discussion

The hydroxylation of $[Li^+@C_{60}](PF_6^-)$ was carried out using the reported procedures under the optimized reaction conditions

[a]*Division of Applied Chemistry, Graduate School of Engineering, Osaka University, 2-1 Yamadaoka, Suita, Osaka 565-0871, Japan. E-mail: kokubo@chem.eng.osaka-u.ac.jp; Fax: +81-6-6879-4593; Tel: +81-6-6879-4592*

[b]*A Research and Analytical Center for Giant Molecules, Graduate School of Science, Tohoku University, 6-3 Aza-aoba, Aramaki, Aoba-ku, Sendai, Miyagi 980-8578, Japan*

† Electronic supplementary information (ESI) available: Experimental details, HPLC chart, ^{13}C NMR, FAB MS, UV-vis, ^{31}P and ^{19}F NMR, and Vis-NIR spectra of compounds. See DOI: 10.1039/c3nr33608e

(Scheme 1). The product was characterized through infrared spectroscopy (IR), nuclear magnetic resonance spectroscopy (NMR), fast atom bombardment mass spectroscopy (FAB MS), thermogravimetric analysis (TGA) as well as the elemental analysis. The IR spectrum of the product is shown in Fig. 1 along with that of the empty fullerenol $C_{60}(OH)_n$ ($n = 10$, as the average structure of a mixture of isomers) synthesized independently by the same fuming sulfuric acid method as a reference. The spectrum showed five characteristic bands at 3281, 1625, 1418, 1081 and 1040 cm^{-1} assignable to νO–H, νC=C, δ_sC–O–H and two types of νC–O, respectively. These absorption peaks clearly confirm the formation of a fullerenol cage. Of interest is that the splitting of the νC–O peak was observed only for Li^+ encapsulated fullerenol. The higher energy band at 1080 cm^{-1} (by *ca.* 40 cm^{-1}) implies the appearance of the fullerenoxide C–O^- bond with enhanced bond order probably because of the deprotonation from one of the OH groups by electrostatic repulsion against the encapsulated Li^+ ion.[20]

The encapsulated lithium cations were clearly detected by ^{7}Li NMR spectroscopy. In the spectrum obtained in DMSO-d_6, three characteristic signals were observed in the range of −15 to −19 ppm relative to LiCl in D_2O as an external standard (Fig. 2a). The observed upfield chemical shifts apparently suggest the encapsulation of Li^+ by the π-conjugated fullerene cage. The abnormal higher upfield shift of the product than that of $[Li^+@C_{60}](SbCl_6^-)$ salt (−10.5 ppm)[1] may be caused by the increased diamagnetic shielding effect of the appeared surface negative charge interacting with the inner lithium cation as already reported in our recent paper.[19] These three sharp signals seem to correspond to a major isomer (−16.7 ppm, *ca.* 70%) and two minor isomers (−15.3 and −18.2 ppm, *ca.* 10 and 20% by integration ratio), respectively. This ^{7}Li NMR spectrum is quite different from the highly broadened previous one,[19] implying the formation of the less number of isomers possibly due to the unusual site-selective hydroxylation. Surprisingly, as shown in Fig. 2b, seven tall sharp peaks (*a–g*) along with four smaller minor peaks (*) assignable to –OH groups were clearly detected by ^{1}H NMR spectroscopy, whereas the empty fullerenol synthesized from pristine C_{60} showed a highly broadened signal centred at 7 ppm on account of the presence of a wide variety of isomers. These sharp peaks were found to disappear by addition of D_2O due to H–D exchange of the hydroxyl protons. The product distribution of isomers was also confirmed by HPLC analysis, consistent with ^{7}Li NMR (Fig. S1†). Whereas the three isomers could be detected clearly, their preparative separation was failed because (1) we could not secure enough amount of starting lithium encapsulated fullerene and (2) the product easily degraded during the separation process.

It was also noted that the ^{13}C NMR spectrum provided several signals assigned for sp^3 C–OH carbons at 72–77 ppm, probably eight large peaks and four small peaks, together with

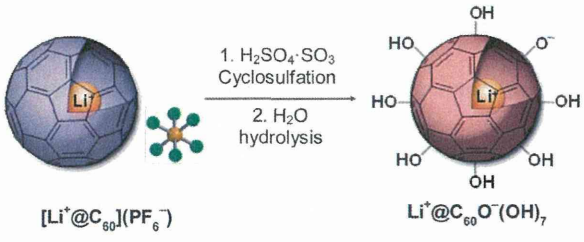

Scheme 1 Synthesis of lithium encapsulated fullerenol.

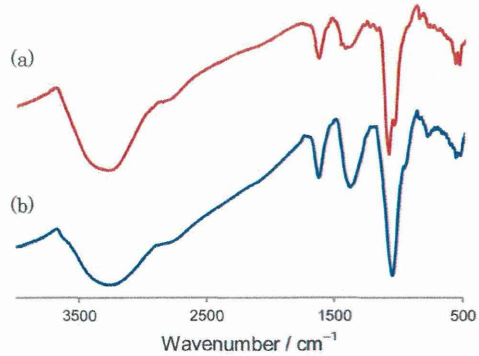

Compound	Absorptions / cm^{-1} (assigned to)			
Product	3281 (νO–H)	1625 (νC=C)	1418 (δ_sC–O–H)	1081, 1040 (νC–O)
$C_{60}(OH)_{10}$	3250	1622	1373	1044

Fig. 1 IR spectra and the typical absorptions (cm^{-1}) of (a) the Li^+ encapsulated fullerenol and (b) reference empty fullerenol $C_{60}(OH)_{10}$.

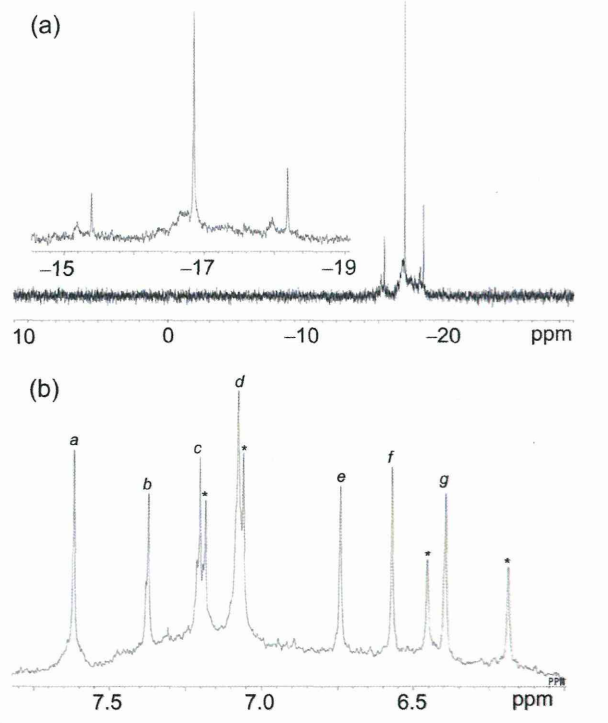

Fig. 2 (a) ^{7}Li NMR spectrum and (b) ^{1}H NMR spectrum of the Li^+-encapsulated fullerenol in DMSO-d_6. The D_2O solution of LiCl was used as an external standard for the measurement of ^{7}Li NMR.

over 40 signals of sp^2 carbons at 140–160 ppm (Fig. S2†), in conformity with the C_1 symmetrical structure. Unfortunately, however, the peaks corresponding to the minor isomers could not be clearly observed due to the small amount of the sample even on 60 000 times accumulation.

Furthermore, we also confirmed the formation of lithium encapsulated fullerenol by positive mode fast atom bombardment mass spectroscopy (FAB MS) (Fig. 3, and the details are shown in Fig. S3†) and UV-vis-NIR spectroscopy (Fig. S4†). The peak at $m/z = 863$ was attributed to $Li^+@C_{60}O^-(OH)_7$, suggesting the encapsulation of the lithium cation. The high resolution matrix-assisted laser desorption ionisation time of flight (MALDI-TOF) mass spectroscopy also showed the molecular ion peak assignable to the same species. The UV-vis-NIR spectrum of the product was essentially the same as that of the empty one. Finally, the structure was deduced from the elemental analysis as being almost the same as the formula of $Li^+@C_{60}O^-(OH)_7 \cdot 4H_2O$ (Table 1).

These findings strongly indicate that the Li^+ encapsulated fullerenols consist of a single major regioisomer (*ca.* 70%) of $Li^+@C_{60}O^-(OH)_7$ which has seven OH groups and one fullerenoxide ($C_{60}O^-$) moiety with C_1 symmetry. Similar to the minor products it may be conceived of having a pair of (1) different regioisomers of the major one or (2) the more or less hydroxylated fullerenols.

Very interestingly, we confirmed that the counter anion PF_6^- was completely lost in the product on the basis of ^{31}P and ^{19}F NMR spectroscopy (Fig. S5 and S6†). This phenomenon can be explained by the formation of a fullerenoxide ($C_{60}O^-$) anion moiety which no longer needs the counter anion such as PF_6^- (*vide supra*). The negative charge of fullerenoxide ($C_{60}O^-$) may be partly dispersed on the highly conjugated fullerene surface on account of the favourable electrostatic interaction with inner Li^+ ions. As a result, the Li^+ would highly be inclined toward one side of the inner wall of C_{60} as similarly reported for $[Li^+@C_{60}](SbCl_6^-)$ (ref. 1) and $[Li^+@PCBM](PF_6^-)$.[3] We have confirmed such Li^+ behavior by DFT calculation as previously reported.[19] Therefore, we propose the structure of $Li^+@C_{60}O^-(OH)_7$ without any free counter anion, and thus the compound could be considered as a "cation encapsulated anion nanoparticle".

Why did the hydroxylation reaction of lithium encapsulated fullerene take place site-selectively? The time course of Vis-NIR spectra of the reaction intermediate in the cyclosulfation step[9] recorded in fuming sulfuric acid $H_2SO_4 \cdot SO_3$ at room temperature provided telling clues about the reason. The spectrum just after the reaction started is shown in Fig. 4 together with the case of empty C_{60} under the same conditions. The broad peak around 823 nm (blue line) in the reaction of empty fullerene with fuming sulfuric acid suggests the generation of divalent cations of C_{60} (C_{60}^{2+}) through the two-electron oxidation which was induced by strong acceptor $H_2S_2O_7$ resulting from SO_3.[21–23] By contrast, the characteristic band of the Vis-NIR spectrum at 964 nm (red line) and the ESR spectrum recorded in fuming sulfuric acid (Fig. 5) for Li^+ encapsulated one indicated that the cation radical ($Li^+@C_{60}^{+\cdot}$) was exclusively produced through one-electron oxidation.[24] The lower g value (2.0016) compared

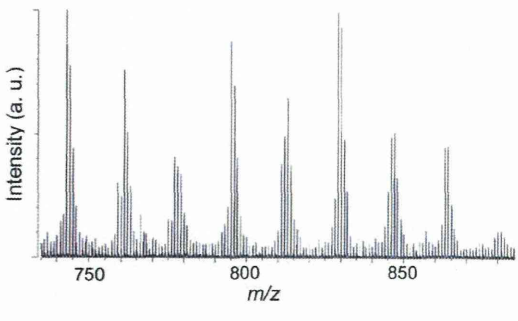

Fig. 3 Positive mode FAB mass spectrum of the product. The peak observed at $m/z = 863$ attributed to $Li^+@C_{60}O^-(OH)_7$ ($M + H^+$) was detected. The other peaks at 743, 761, 777, 795, 811, 829, and 845 were fragment signals assignable to $LiC_{60}O(OH)_{0-6}$, respectively.

Table 1 Elemental analysis of the product

Average structure	Elemental analysis[a] (%)	Water content[a,b] (wt%)
Product	C: 77.16, H: 1.84	5.1
$Li@C_{60}O(OH)_7 \cdot 4H_2O$	(C: 77.10, H: 1.62)	(7.7)

[a] Values in parentheses are calculated data. [b] Water content was determined by TGA.

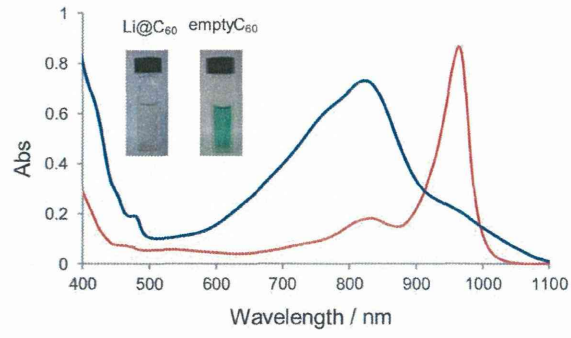

Fig. 4 Vis-NIR spectra of the reaction intermediate during the cyclosulfation of $[Li^+@C_{60}](PF_6^-)$ (red) and empty fullerene (blue) in fuming sulfuric acid. Inset: the visual color of the solutions.

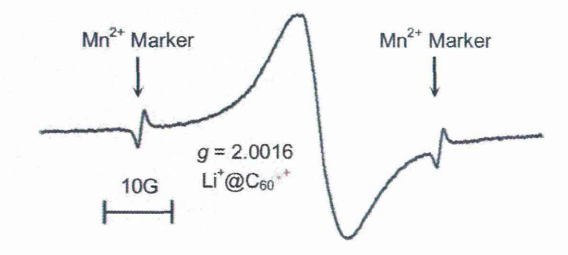

Fig. 5 ESR spectrum of the reaction intermediate during the cyclosulfation of $[Li^+@C_{60}](PF_6^-)$ recorded in fuming sulfuric acid at 298 K calibrated by using a Mn^{2+} marker.

with the reported empty C_{60} radical cation and the line broadening was probably due to the polarity of fuming sulfuric acid and internal lithium cation.[25–27]

These differences in the ionization potential between the Li^+ encapsulated C_{60} and the empty one can be rationalized by comparing their UV-vis spectra as well as reduction potentials. The UV-vis spectra of these fullerenes are almost superimposable, because of essentially the same HOMO–LUMO energy gaps. However, the first reduction potential, which corresponds to LUMO, of Li^+ encapsulated C_{60} was found to be 0.7 V more reducible than the empty one on cyclic voltammetry (CV) measurement.[1] Therefore, the first oxidation potential which corresponds to the HOMO should also be different by *ca.* 0.7 V due to the strong electron accepting ability of Li^+ and thus monovalent $Li^+@C_{60}^{+\cdot}$ seems to be sluggishly formed on fuming sulfuric acid oxidation, while the empty C_{60} can be easily oxidized to the divalent cation species.[21–23] Indeed, monovalent cation radical $Li^+@C_{60}^{+\cdot}$ was found to be persistent several days in fuming sulfuric acid, whereas the divalent one degraded within several hours. Therefore, the cyclosulfation reaction of $[Li^+@C_{60}](PF_6^-)$ was quite slow as compared with the reaction of the empty one (see Fig. S7–S9†). This difference in the stability (*i.e.*, reactivity) of the oxidized species is partly responsible for the difference in the site-selectivity of the multi-step addition of fuming sulfuric acid.[28–30] The Vis-NIR spectrum of the reaction intermediate of the "Li@C_{60} cluster"[19] in fuming sulfuric acid was also recorded for comparison (Fig. S10†). However, no clear peak at ~960 nm which can be seen in the case of $[Li^+@C_{60}](PF_6^-)$ was observed probably due to the heterogeneous cluster nature of $Li^+@C_{60}^{-\cdot}$ surrounded by neutral C_{60} molecules. This electronic difference as well as the steric restriction could result in the unselective hydroxylation of the Li@C_{60} cluster.[19]

One of the effects of the introduced hydroxyl groups to $[Li^+@C_{60}](PF_6^-)$ was the improvement of solubility. Although the solubility of $[Li^+@C_{60}](PF_6^-)$ is low compared with pristine C_{60}, $Li^+@C_{60}O^-(OH)_7$ could be dissolved in polar solvents such as DMSO and DMF comparable with the empty one. Indeed, the particle size analysis by the induced grating (IG) method[31] showed the small and narrow particle size distribution (*ca.* 1.1 nm, original molecular size) in DMSO solution (Fig. 6). The size was also confirmed by scanning prove microscopy (SPM) for the sample prepared by applying the highly diluted aqueous solution of fullerenol to a mica plate and drying it (Fig. 6).

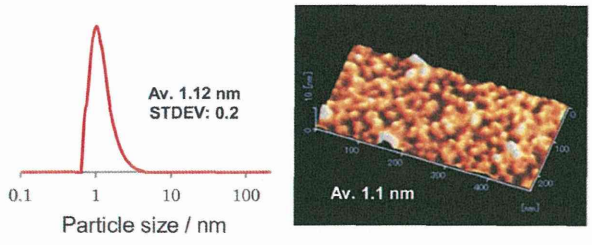

Fig. 6 Particle size distribution of $Li^+@C_{60}O^-(OH)_7$ in DMSO solution (1 mM) measured by the IG method (left) and SPM particle size analysis for $Li^+@C_{60}O^-(OH)_7$ on a mica plate (right).

Conclusions

In summary, we synthesized $Li^+@C_{60}O^-(OH)_7$ using a fuming sulfuric acid method from $[Li^+@C_{60}](PF_6^-)$ and characterized its structure by IR, NMR and FAB mass spectroscopy as well as the elemental analysis. Notably, the reaction of $[Li^+@C_{60}](PF_6^-)$ was site-selective to give a single major isomer (*ca.* 70%) with two minor isomers in marked contrast to the case of the Li@C_{60} cluster. We concluded from the analysis of radical species produced in the reaction of fuming sulfuric acid and C_{60} cage that this unusual site-selective hydroxylation was caused by the lower HOMO level of lithium encapsulated fullerene than that of empty C_{60}. This result suggests the possibilities of the metal encapsulated fullerenes being capable of becoming a new-type of fullerene multi-adducts with appreciable site-selectivity. Further mechanistic investigation on site-selectivity and the properties of $Li@C_{60}^{+\cdot}$ are now undertaken as well as the application of our new Li^+ encapsulated fullerene compounds.

Experimental section

Synthesis of $Li^+@C_{60}O^-(OH)_7$

A slurry of $[Li^+@C_{60}](PF_6^-)$ (10 mg, 12 μmol) in 30% fuming sulfuric acid (0.5 mL) was stirred for 48 h at 60 °C under an Ar atmosphere. After cooling to room temperature, the resulting mixture was added dropwise into chilled diethyl ether (100 mL). After centrifugation, the residual solid was washed three times with *ca.* 10 mL of diethyl ether and dried under vacuum at 30 °C. The resulting brown solid was added to water (3 mL) and the mixture was stirred for 48 h at 70 °C in air. After cooling to room temperature, the suspension was filtered and the residual solid was washed with water until the solution was neutralized (40 mL). It was then washed three times with acetonitrile and diethyl ether (40 mL each) and dried under vacuum at 40 °C for 24 h, resulting in $Li^+@C_{60}O^-(OH)_7 \cdot 4H_2O$ (9.2 mg, 9.9 μmol, 83%) as a brown powder.

Acknowledgements

This work was supported by Grant-in-Aid for Exploratory Research (no. 23651111) from JSPS, Japan, and Health Labour Sciences Research Grants from MHLW, Japan. The authors thank Nacalai Tesque Inc. for the helpful guidance of HPLC analysis.

References

1 S. Aoyagi, E. Nishibori, H. Sawa, K. Sugimoto, M. Takata, Y. Miyata, R. Kitaura, H. Shinohara, H. Okada, T. Sakai, Y. Ono, K. Kawachi, K. Yokoo, S. Ono, K. Omote, Y. Kasama, S. Ishikawa, T. Komuro and H. Tobita, *Nat. Chem.*, 2010, **2**, 678–683.

2 (*a*) S. Fukuzumi, K. Ohkubo, Y. Kawashima, D. S. Kim, J. S. Park, A. Jana, V. M. Lynch, D. Kim and J. L. Sessler, *J. Am. Chem. Soc.*, 2011, **133**, 15938–15941; (*b*) K. Ohkubo, Y. Kawashima and S. Fukuzumi, *Chem. Commun.*, 2012, **48**, 4314–4316.

3 Y. Matsuo, H. Okada, M. Maruyama, H. Sato, H. Tobita, Y. Ono, K. Omote, K. Kawachi and Y. Kasama, *Org. Lett.*, 2012, **14**, 3784–3787.

4 L. Y. Chiang, F.-J. Lu and J.-T. Lin, *J. Chem. Soc., Chem. Commun.*, 1995, 1283–1284.

5 H. Aoshima, K. Kokubo, S. Shirakawa, M. Ito, S. Yamana and T. Oshima, *Biocontrol Sci.*, 2009, **14**, 69–72.

6 J. Gao, L. Wang, K. M. Folta, V. Krishna, W. Bai, P. Indeglia, A. Georgieva, H. Nakamura, B. Koopman and B. Moudgil, *PLoS One*, 2011, **6**, e19976.

7 Y. Saitoh, H. Mizuno, L. Xiao, S. Hyoudou, K. Kokubo and N. Miwa, *Mol. Cell. Biochem.*, 2012, **366**, 191–200.

8 Z. Chen, L. Ma, Y. Liu and C. Chen, *Theranostics*, 2012, **2**, 238–250.

9 L. Y. Chiang, L.-Y. Wang, J. W. Swirczewski, S. Soled and S. Cameron, *J. Org. Chem.*, 1994, **59**, 3960–3968.

10 N. S. Schneader, A. D. Darwish, H. W. Kroto, R. Taylor and D. R. M. Walton, *J. Chem. Soc., Chem. Commun.*, 1994, 463–464.

11 S. Wang, P. He, J.-M. Zhang, H. Jiang and S.-Z. Zhu, *Synth. Commun.*, 2005, **35**, 1803–1807.

12 A. Arrais and E. Diana, *Fullerenes, Nanotubes, Carbon Nanostruct.*, 2003, **11**, 35–46.

13 J. Li, A. Takeuchi, M. Ozawa, X. Li, K. Saigo and K. Kitazawa, *J. Chem. Soc., Chem. Commun.*, 1993, 1784–1785.

14 K. Kokubo, K. Matsubayashi, H. Tategaki, H. Takada and T. Oshima, *ACS Nano*, 2008, **2**, 327–333.

15 K. Kokubo, S. Shirakawa, N. Kobayashi, H. Aoshima and T. Oshima, *Nano Res.*, 2011, **4**, 204–215.

16 G. Zhang, Y. Liu, D. Liang, L. Gan and Y. Li, *Angew. Chem., Int. Ed.*, 2010, **49**, 5293–5295.

17 M. Mikawa, H. Kato, M. Okumura, M. Narazaki, Y. Kanazawa, N. Miwa and H. Shinohara, *Bioconjugate Chem.*, 2001, **12**, 510–514.

18 B. Sitharaman, R. B. Bolskar, I. Rusakova and L. J. Wilson, *Nano Lett.*, 2004, **4**, 2373–2378.

19 H. Ueno, Y. Nakamura, N. Ikuma, K. Kokubo and T. Oshima, *Nano Res.*, 2012, **6**, 558–564.

20 R. H. Seubold, Jr, *J. Org. Chem.*, 1956, **21**, 156–160.

21 H. Thomann, M. Bernardo and G. P. Miller, *J. Am. Chem. Soc.*, 1992, **114**, 6593–6594.

22 F. Cataldo, *Spectrochim. Acta*, 1995, **51A**, 405–414.

23 S. P. Solodovnikov, *Russian Chemical Bulletin*, 1998, **47**, 2302–2304.

24 R. D. Webster and G. A. Heath, *Phys. Chem. Chem. Phys.*, 2001, **3**, 2588–2594.

25 S. G. Kukolich and D. R. Huffman, *Chem. Phys. Lett.*, 1991, **182**, 263–265.

26 S. Fukuzumi, T. Suenobu, T. Urano and K. Tanaka, *Chem. Lett.*, 1997, 875–876.

27 K. Tanaka, H. Ago, Y. Matsuura, T. Kuga, T. Yamabe, S. Yuda, Y. Hato and N. Ando, *Synth. Met.*, 1997, **89**, 133–139.

28 C. D. Johnson, *Chem. Rev.*, 1975, **75**, 755–765.

29 B. Giese, *Angew. Chem., Int. Ed. Engl.*, 1977, **16**, 125–136.

30 A. Pross, in *Advances in Physical Organic Chemistry*, ed. V. Gold and D. Bethell, Academic Press, London, New York, San Francisco, 1977, vol. 14, p. 69–132.

31 Y. Wada, S. Totoki, M. Watanabe, N. Moriya, Y. Tsunazawa and H. Shimaoka, *Opt. Express*, 2006, **14**, 5755–5776.